Supplementary information

Enhanced Thermoelectric Performance of $Ca_3Co_4O_9$ Ceramics through Grain Orientation and Interface Modulation

Zongmo Shi[1], Taichao Su[2], Ping Zhang[1], Zhihao Lou[1], Mengjie Qin[1], Tong Gao[3], Jie Xu[1, 4], Jihong Zhu[3], and Feng Gao[1]*

1 State Key Laboratory of Solidification Processing, MIIT Key laboratory of Radiation Detection Materials and Devices, USI Institute of Intelligence Materials and Structure, NPU-QMUL Joint Research Institute of Advanced Materials and Structure, School of Material Science and Engineering, Northwestern Polytechnical University, Xi'an, 710072, P. R. China

2 School of Materials Science and Engineering, Henan Polytechnic University Jiaozuo, 454003, P. R. China

3 State IJR Center of Aerospace Design and Additive Manufacturing, MIIT Lab of Metal Additive Manufacturing and Innovative Design, Northwestern Polytechnical University, Xi'an, 710072, P. R. China

4 Research & Development Institute of Northwestern Polytechnical University in Shenzhen, Shenzhen, 518057, P. R. China

[*] Corresponding author:

F. Gao, E-mail address: gaofeng@nwpu.edu.cn

Figure S1 shows the XRD patterns of template seeds and precursor powders. Both of the two patterns could be indexed as the single-phase CCO without any secondary phases (PDF# 21-0139, space group: *C*2/m). All the main diffraction peaks of template seeds corresponded well to PDF card, and a preferred orientation was observed. In addition, an obvious diffraction peak of $(20\bar{1})$ plane appeared and located at 37.2° for the $(Ca_{0.87}La_{0.03}Ag_{0.1})_3Co_4O_9$ powders. The inserted SEM image shows the morphologies of template seeds and precursor powders.

Figure S2 shows the distributed sizes of precursor powders with different ball-milling time. It can be seen that the particles sizes of the powders decreased slightly when the ball-milling time reached 36 h before. While the two different sizes of particles could be observed after 48 h and it met the need of TGG process.

In order to obtain the precursor powders with high surface energy, the precursor powders were milled for a long time. Figure S3 shows the BET results of precursor powders milled 48 h. The specific surface area of 2.25 m^2/g was obtained for the precursor powders from the BET result. It has been illustrated that a satisfactory submicron size of precursor powders and an ideal morphology of template seeds could be used to prepare textured ceramics with a large difference surface energy.

Figure S4 shows the schematic diagram of TGG process. Highly textured and anisotropic CCO ceramics were prepared using tape casting technology. The organic additives of polyvinyl butyral binder, adjacent dioctyl phthalate plasticizer, and castor oil lubricant and xylene-ethanol solvent were mixed accompanying with CALC matrix powders. The CCO template seeds of 20 wt% were added into the slurry and ball milled for 48 h. The homogeneous slurry was tape casted through the gated doctor blade and the thick film of 30 μm was obtained. The multilayered sheets were cut into 100

mm×100 mm and laminated a green body with the height of 4 mm and 15 mm. The hot water pressure was implemented to the bulks.

Figure S5 and Figure S6 show the reverse pole figures and ODF for the textured samples. The polar maps evidenced the strongly preferred orientation of the textured samples. In contrast, the counterpart without template seeds was the random orientation of the grains.

To illustrate Ag incorporation, the high-resolution XPS spectra for Ag 3*d* of the 1373 K sample was performed, as shown in Figure S7. In comparison to the standard XPS spectra of sliver [S1], the positions of Ag $3d_{5/2}$ and Ag $3d_{3/2}$ spectra yielded two peaks at 367.9 eV and 373.9 eV, indicating the existence of metallic Ag and lattice Ag^+. **Table** S1 shows the relative content about Ag^+ and metallic Ag segregation for all samples. It shows that with the increasing of sintering temperature, the relative content of metallic Ag slightly varied, suggesting that it could accelerate the transport of charge carriers.

References:

[S1] C. C. Han, L. Ge, C. F. Chen, Y. J. Li, Z. Zhao, X. L. Xiao, Z. L. Li and J. L. Zhang, Site-selected synthesis of novel Ag@AgCl nanoframes with efficient visible light induced photocatalytic activity, *J. Mater. Chem. A,* 2014, 2, 12594-12600.

List of Tables in Supplementary Information

Table R1 Concentration of sliver states for the XPS fitting results.

Relative content/%	without seeds	1173 K	1273 K	1373 K
Ag^+	92.7	91.2	92.5	91.9
metallic Ag	7.3	8.8	7.5	8.1

List of Figures in Supplementary Information

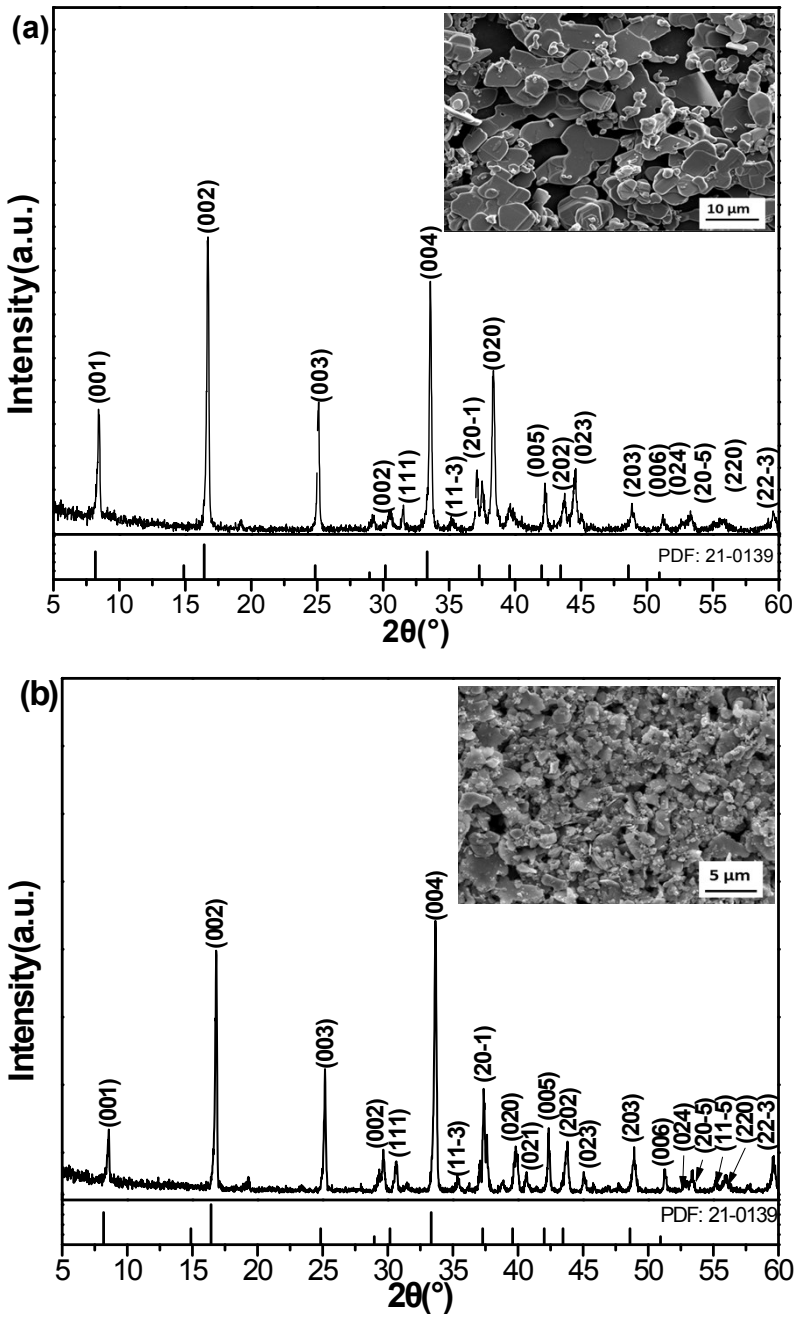

Figure S1 XRD patterns and SEM micrographs of template seeds and precursor powders. (a) template seeds, (b) precursor powders

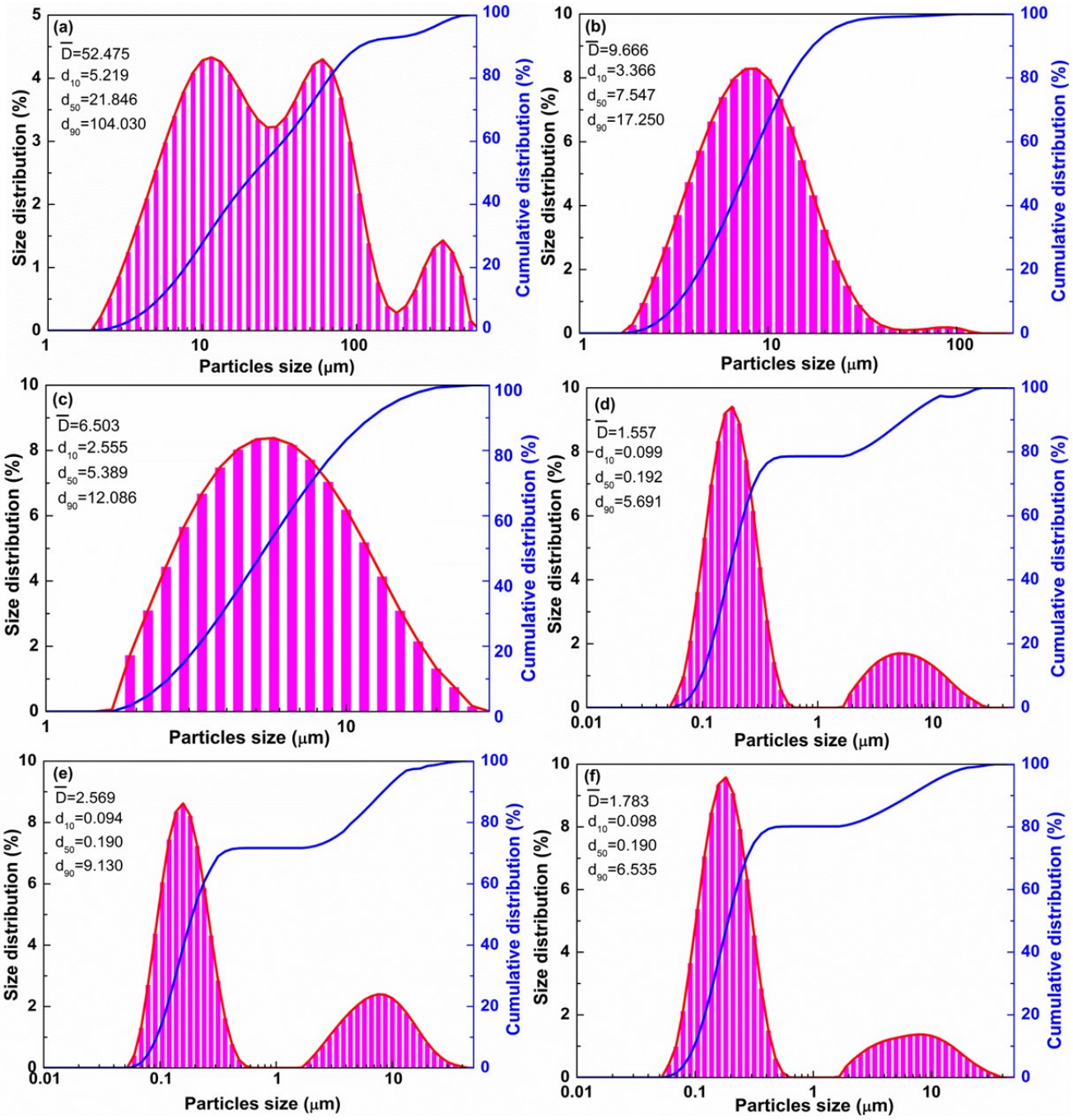

Figure S2 Particle sizes of precursor powders with different ball-milling time. (a) 12 h, (b) 24 h, (c) 36 h, (4) 48 h, (e) 60 h, (f) 72 h

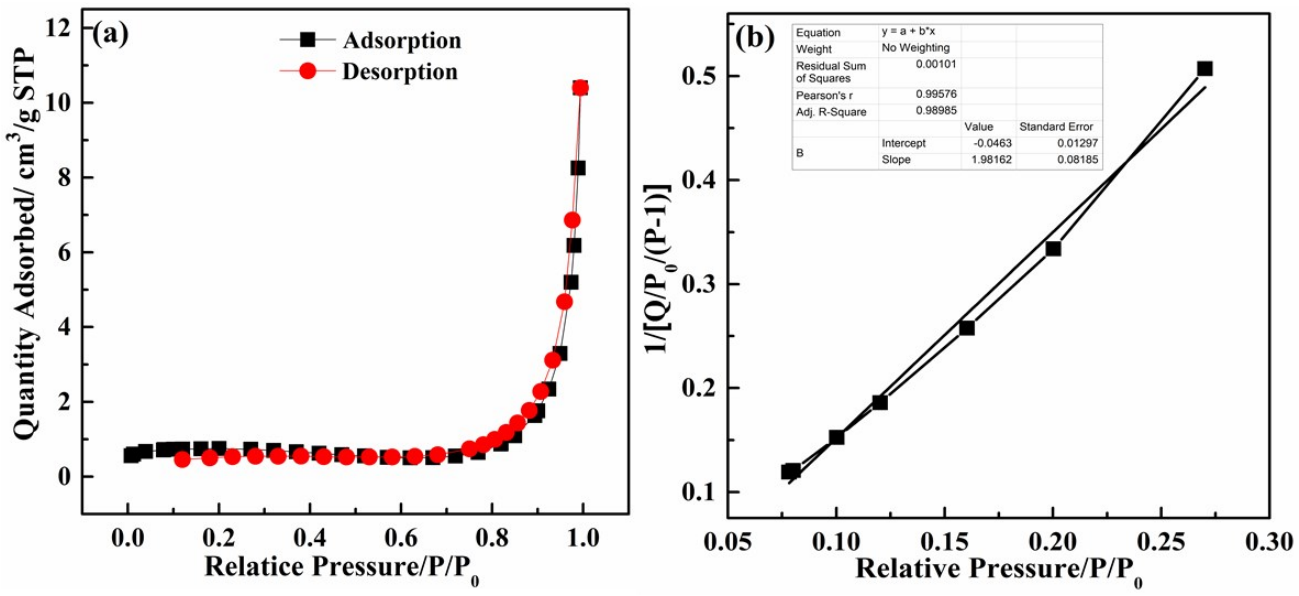

Figure S3 BET result for precursor powders milled 48 h. (a) adsorption-desorption curve, (b) specific surface area

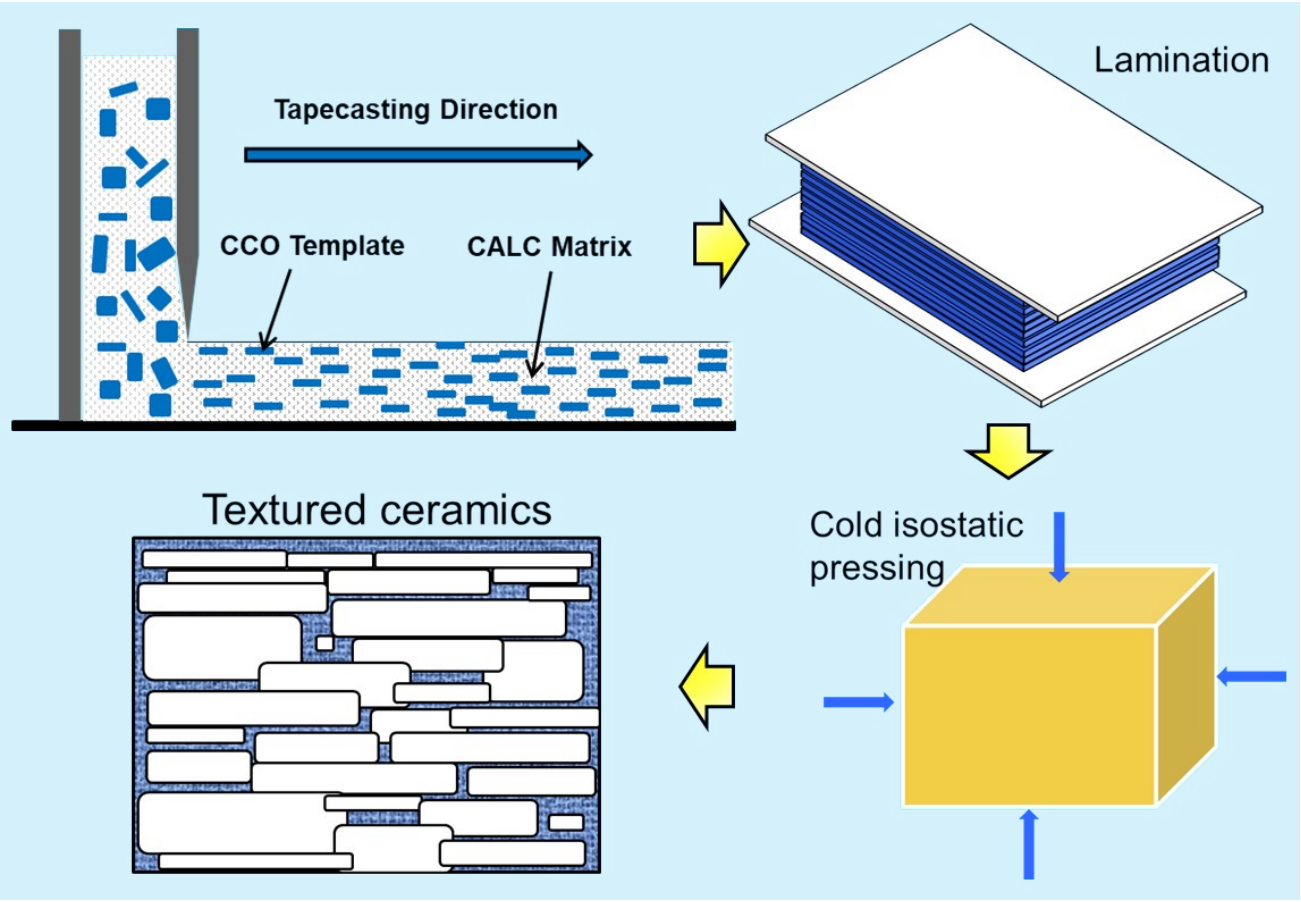

Figure S4 Schematic diagram of TGG process.

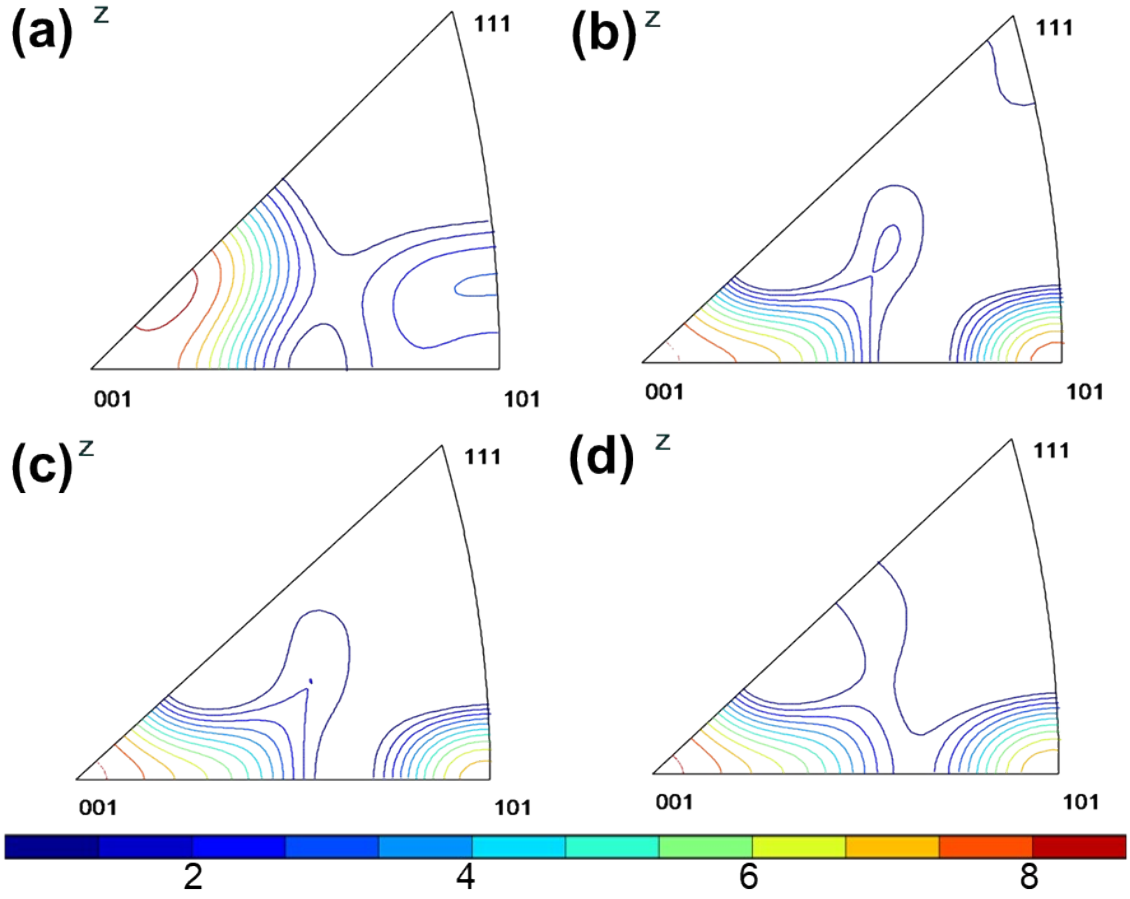

Figure S5 Reverse pole figures for the textured samples. (a) without CCO seeds, (b) 1173 K, (c) 1273 K, (d) 1373 K

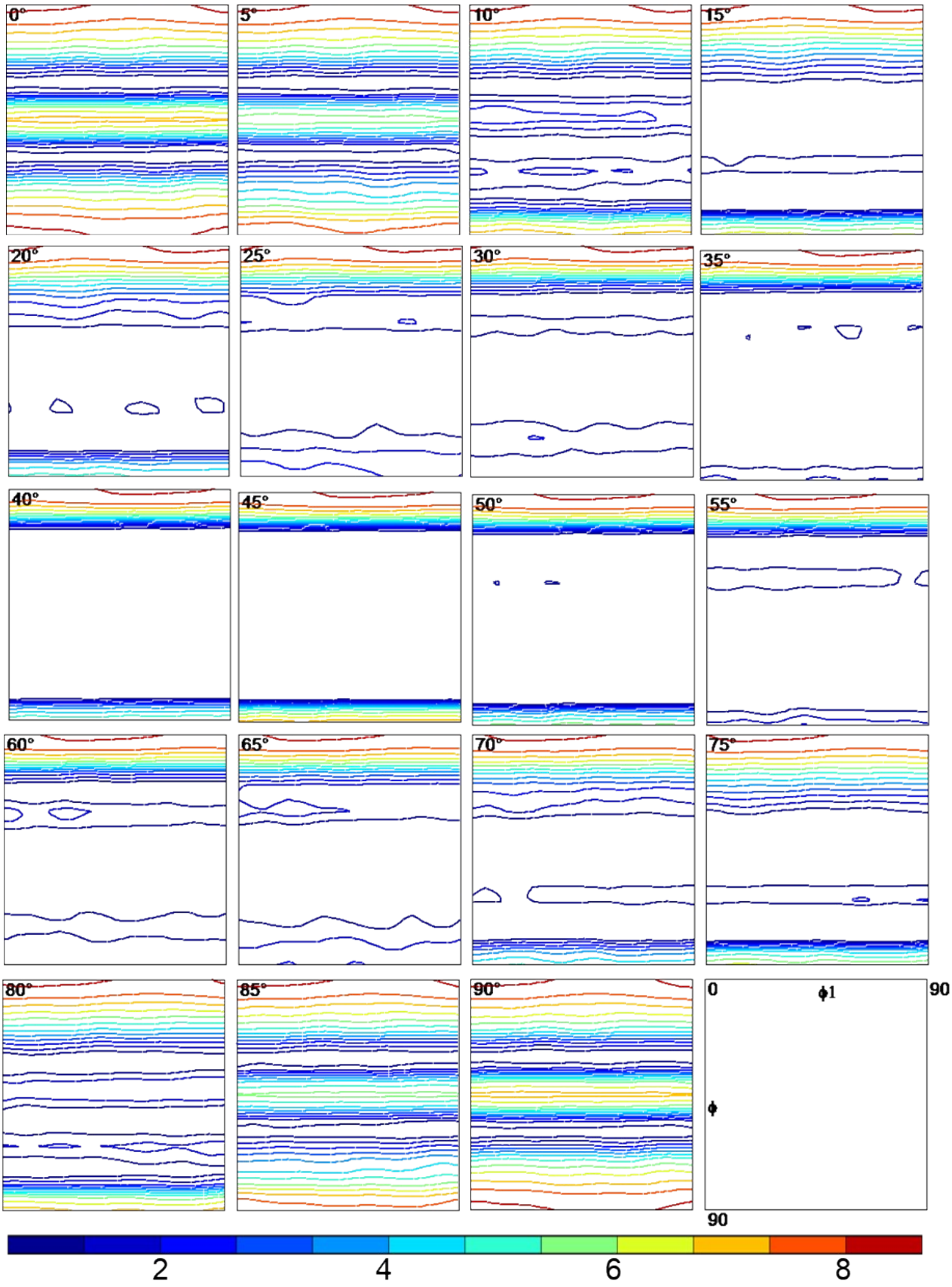

Figure S6 Refined orientation distribution function (ODF) for the 1373 K sample.

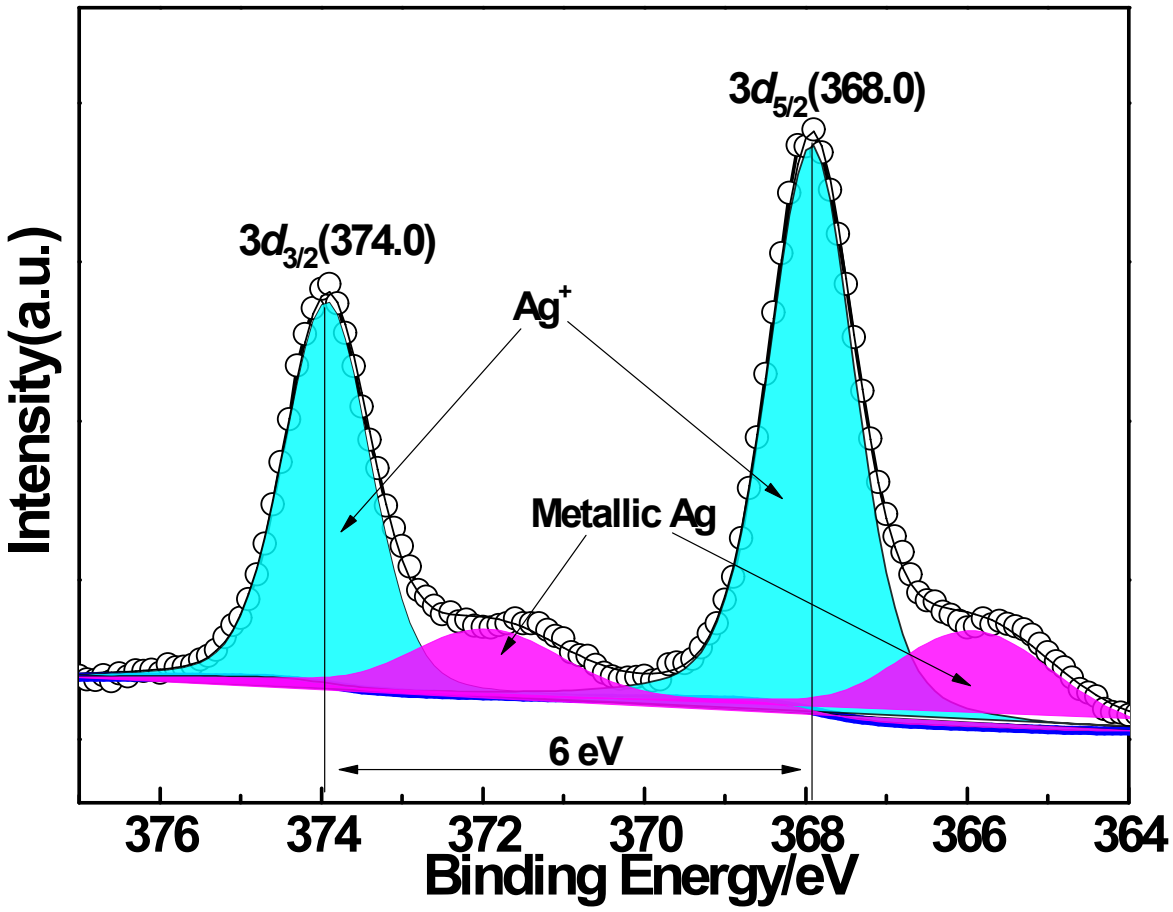

Figure S7 High-resolution Ag 3*d* spectra for the 1373 K sample.